ROZPRAWY INŻYNIERSKIE • ENGINEERING TRANSACTIONS • 32, 4, 523–535, 1984
Polska Akademia Nauk • Instytut Podstawowych Problemów Techniki

THE INFLUENCE OF DIRECTION AND VALUE OF PLASTIC PRESTRAIN ON STEADY-STATE CREEP RATE USING THE COMBINED ISOTROPIC-KINEMATIC HARDENING RULE

M. WANIEWSKI (WARSZAWA)

The effect of changing in direction and value of room temperature plastic prestrain on steady-state creep rate is experimentally investigated by applying combined loadings of axial and shear forces to the pure copper thin-walled tubular specimens. The constitutive equation is verified by employing the two different approaches — the notation of creep plastic potential and the properties of tensor functions representation.

1. Introduction

Applied technological plastic treatment in the process of forming elements of turbines, jet engines and reactor induces anisotropy for materials subjected further to effect long-term, constant stress levels at elevated temperature conditions.

Preliminary plastic deformation has an influence on such material creep properties as time and strain rupture, also on the value of steady-state creep rate.

The effect of uniaxial room temperature prestrain upon the subsequent life time and strain rupture on Nimonic 80A has been studied in axial tension creep tests at 750°C by Dyson and Rodgers [1] and in pure torsion conditions by Dyson, Loveday and Rodgers [2] and by Hayhurst, Trąmpczyński and Leckie [3]. The authors [1, 2, 3] proved that the creep rates for prestrained Nimonic 80*A* are increased and life-time is reduced.

Trąmpczyński [4] tested flat specimens by cutting from the sheet of pure copper under different directions to the prestrained direction Szczepiński [5] applied the experimental method.

The author [4] proved that the steady-state creep rates for prestrained pure copper are decreased and the degree of material creep hardening depends on the direction and value of plastic prestrain.

Hayhurst, Trąmpczyński and Leckie [3] utilizing the experimental data [1, 2] verified the influence of the value of plastic prestrain on life-time; they used the theory in which the increase of the value of the creep damage parameter is explained by two simultaneous processes — nucleation and growth of voids.

TRĄMPCZYŃSKI [4] applied the notation of creep plastic potential introduced by RICE [6] and described the creep anisotropy using isotropic-kinematic hardening parameters.

The tensor functions representation is a different description of influence of strain-induced anisotropy on creep performed by SAWCZUK, TRĄMPCZYŃSKI [7] — this approach is based on the theory of plasticity for anisotropic materials developed by BOEHLER, SAWCZUK [8].

MOZAROWSKI, ANTIPOW and BOBYR [9] described the experiments carried out on steel thin-walled tubular specimens preliminarily prestrained and subsequently subjected to creep under multiaxial states of stress.

2. MATERIAL, SPECIMEN AND TESTING MACHINE

The influence of direction and value of plastic prestrain was studied in pure, electrolytic copper thin-walled tubular specimens subjected to the tension-torsion load system.

Prior to mechanical treatment, the rods were annealed for 2h at 400°C and the furnace was cooled to achieve a uniform grain size.

The tubular specimen was designed to have a constant internal diameter equal to 16 mm, 17.5 mm outer gauge diameter, 160 mm total length and 70 mm gauge length which is limited by circumferential extensometer protrusions.

The tension-torsion creep testing machine incorporates two independent load systems — a lever system for applying tensile loading and a pulley system for applying torsional loading, Fig. 1.

The thin-walled specimen *1* is pinned to two vertical rods. The upper rod *2* is connected through the torque disc *6* to the horizontal lever *9* via a universal joint *4*, Fig. 1. In order to minimize friction, the horizontal lever *9*, which has a mechanical advantage 1:5.5, is supported on a knife edge *10* and connected with the weight hanger *18* and specimen load train through similar knife edges *10* and *12*, Fig. 1.

The testing machine has an automatic device *13* for control position of the horizontal lever *9*, Fig. 1.

Torque is applied to the test piece *1* through the torque dis *6* rotated by steel wires which pass over a system of pulleys *15* to the load hangers *16* and *17*, Fig. 1. In order to minimize friction, all the pulleys are mounted on single row ball bearings. The torque disc *6* is an integral part of the double row ball bearing *7* which minimizes the resistance imposed by the axial load system when twisting couples are applied.

The machine contains a load cell *8* which is located outside the furnace *14*, as a thin-walled tube, Fig. 1. The three-direction oriented strain gauge ele-

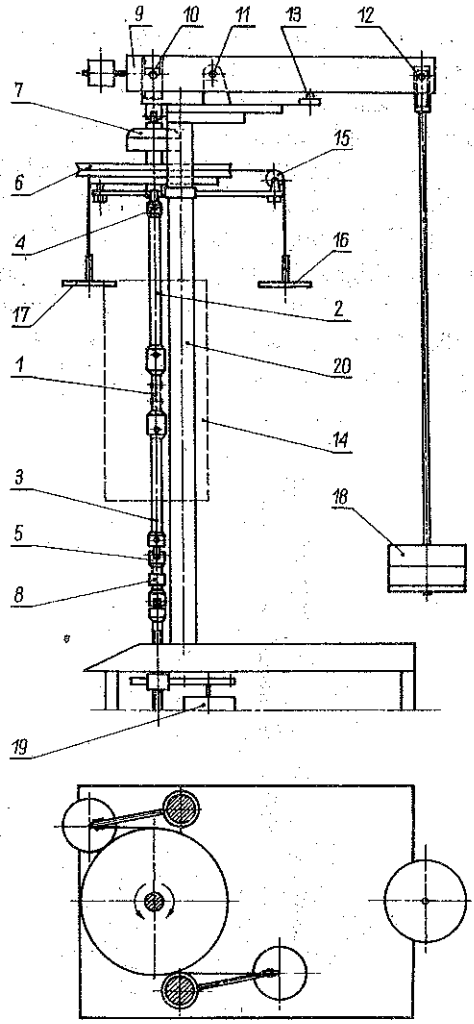

Fig. 1. Diagram of elevated temperature creep testing machine.
1 — Specimen, *2* — upper loading rod, *3* — lower loading rod, *4, 5* — universal joints, *6* — — torque disc, *7* — double ball bearing, *8* — load cell, *9* — horizontal lever, *10, 11, 12* — knife edges, *13* — control equipment, *14* — furnace, *15* — pulleys, *16, 17, 18* — load hangers, *19* — — electric angine.

ments (longitudinal, circumferential and 45° diagonal) allow to compare the actual level of stress state obtained on the specimen gauge surface.

The temperature of the specimen is increased by heat conduction. Heat is supplied by three-sectional heating coils and can be regulated by means of heat conduction alone along the axis of the specimen. Two termocouples were connected to control the data system which allows to keep the temperature constant with an exactitute of ± 1°C in the range up to 900°C.

The temperature at two points located on the specimen gauge surface was automatically recorded on the paper tape.

The testing machine was designed around a mechanical system for measuring the elongation and angle of twist. The extensometer, Fig. 2, consists of inner *3* and *2* tubular members attached respectively to the lower and upper protrusions of the test specimen *1*. The lower ends of tubular members are located outside the furnace. In this place four linear variable differntial transformers (l.v.d.t.) capable of measuring strains with high sensitivity over the travel of ± 10 mm was attached. Two of them, *6* and *7*, measured the angle of twist and the others, *8* and *9*, the axial tension of the gauge surface of the specimen, Fig. 2. To overcome the

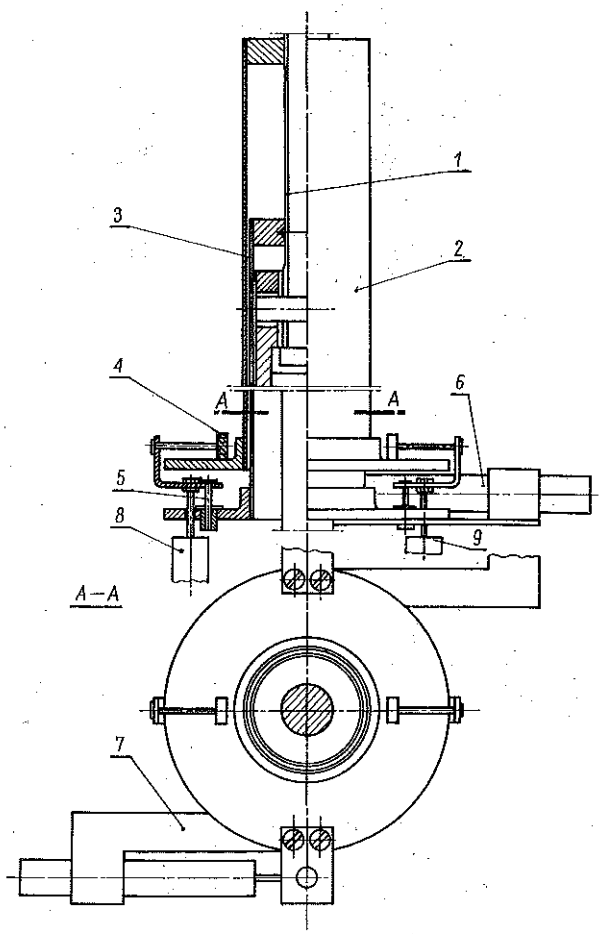

Fig. 2. Cross-section of mechanical extensometer system.
1 — Specimen, *2* — outer extensometer tube, *3* — inner extensometer tube, *4* — ball bearing, *5* — guide pin, *6*, *7* — horizontal l.v.d.t., *8*, *9* — vertical l.v.d.t.

effect of friction between the transducer cores and reference surfaces, it was necessary to isolate the relative axial and torsional motions between two lower ends of the extensometer tubes. To achieve this aim, a mechanical device was used, which consisted of teflon bearings, *4* and *5*, Fig. 2.

Electrical signals obtained from l.v.d.t. are registred on paper tape in arbitrary time intervals. The procedure is described in detail by WANIEWSKI [10].

The results of preliminary tests of the machine and extensometer proved that the design is satisfactory [10].

3. EXPERIMENTAL PROCEDURE

The experiment which consists of two parts was carried out on pure copper thin-walled tubular specimens subjected to the combined tension--torsion load [10].

Under that plane and proportional stress conditions, the response of material in ILYUSHIN [11] subspace $(e_1^p, e_3^p) = [e_{11}^p, (4/3)\, e_{12}^p]$, where e_{11}^p denotes the deviatoric part of the plastic axial prestrain tensor and e_{12}^p denotes the deviatoric part of the plastic shear prestrain tensor, can be described in terms of two parameters, the value $|\bar{e}| = J_2^{1/2} = e_i^p = [e_{11}^p)^2 + (4/3)\,(e_{12}^p)^2]^{1/2}$ and the direction $\theta^p = \operatorname{arc\,tg}\left[2e_{12}^p/\sqrt{3}\, e_{11}^p\right]$ of the prestrain vector $\bar{e}$, where J_2 denotes the second invariant of the prestrain deviator.

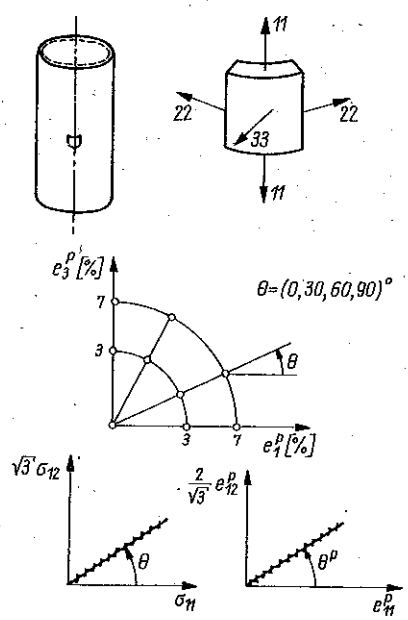

Fig. 3. Programme of room temperature plastic prestrain.

For $\theta^p = (0, 30, 60, 90)°$, two series of thin-walled tubular specimens up to 3% and 7% of plastic prestrain intensity e_i^p, were proportionally deformed at room temperature, Fig. 3.

The results of plastic prestrain are shown in Fig. 4, in dependence form of seconds invariants of the stress vector, σ_i versus the prestrain vector, e_i^p. The discrepancy obtained between the curves, respectively, where the angle θ^p is the parameter, can be explained for the initially isotropic material by the effect of the third invariant stress deviator.

The phenomenon described below was examined by OHASHI, TOKUDA, YAMASHITA [12] who eliminated the eliminated the effect of the third invariant by modifying the two-dimensional vector space. In general, this has been extended to the situation involving five-dimensional vector space. A similar effect, as shown on the plot σ_i vs e_i^p, for plastically deformed thin-walled tubular specimens under multiaxial states of stress has been observed by the investigators MOZAROWSKI, ANTIPOW, BOBYR [9].

In the second part of the experiment the influence of the value and direction of plastic prestrain on steady-state creep rate was investigated.

For this purpose each plastically prestrained specimen was unloaded and heated up to 300°C. After 24 hours the test pieces were subjected to the creep uniaxial stress leael, equal for each specimen, $\sigma_{11}^c = 49$ MPa in the time interval $t = 200$ h, which was sufficiently long to appoint the value of steady, state creep rate.

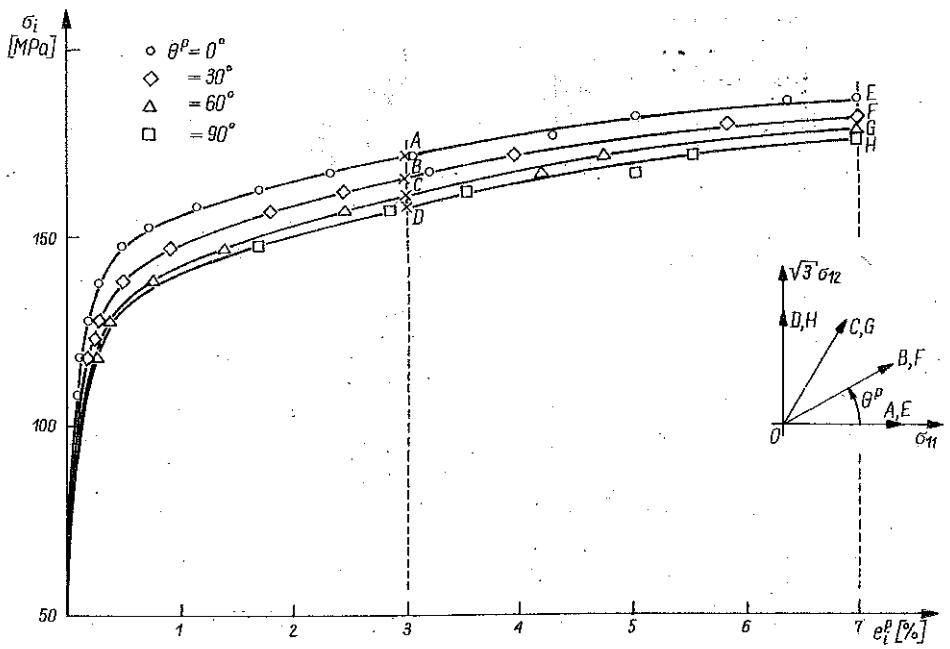

Fig. 4. Material curves.

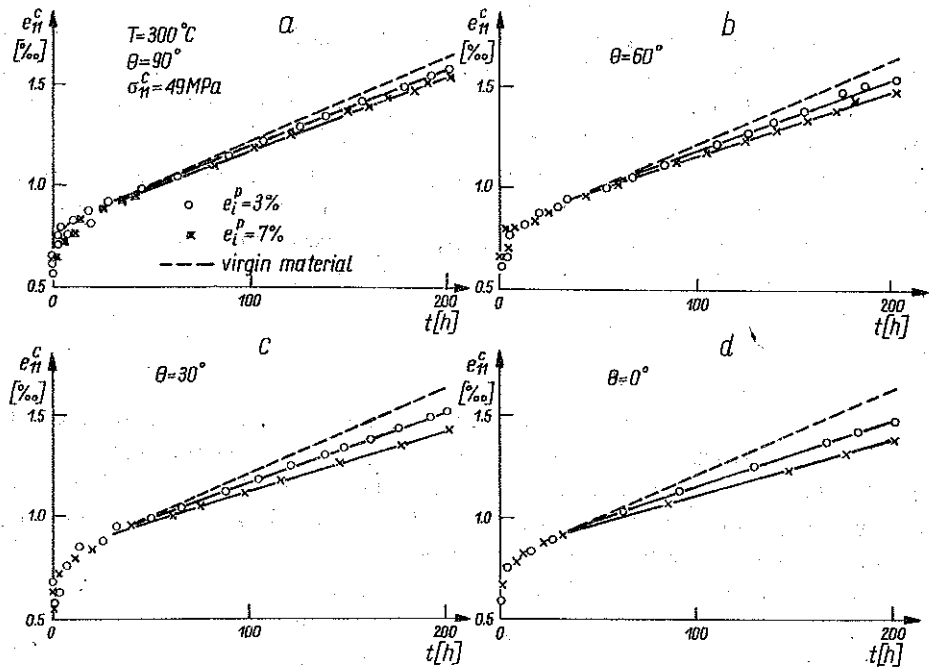

Fig. 5. Creep curves as a function of the angle θ^p and magnitude e_l^p of strain-induced anisotropy.

The value of steady-state creep rate for a material with room temperature biaxial strain-induced anisotropy in comparison with the value of a steady-state creep rate obtained for virgin material (interruption line) tested under the same stress level and at the same temperature are shown Fig. 5.

The obtained values of steady-state creep rates depend on both the magnitude and direction of plastic prestrain, Fig. 5.

4. Theoretical description

Experimental results are discussed by applying the creep potential ideas and the tensor functions representation in terms of two internal state variables, the so-called back stress and drag stress.

The anisotropic creep process described by two internal state variables was developed among others by Rice [6], Miller [13] and Poter, Leckie [14],

$$D_{ij} = f\left(\frac{S_{ij}^c - \alpha_{ij}}{\mathbf{R}}\right), \tag{1}$$

where D_{ij} denotes the deviatoric part of the steady-state creep rate tensor, S^c_{ij}—the deviatoric part of the creep stress tensor, α_{ij}—the tensor state variable, called drag stress and R—the scalar state variable, called back stress; both state variables depend on the previous deformation history.

From the results of the current experiment it follows that a material with room temperature plastic prestrain has an anisotropic character and steady-state creep rate can be described by using two internal state variables α_{ij} and R, [4, 10]

$$\frac{D_{ij}}{D_0} = \frac{3}{2}(\Phi)^{n-1} \times \frac{S^c_{ij} - \alpha_{ij}}{R\sigma_0}, \tag{2}$$

where Φ denotes the scalar function dependent on the second and third stress tensor invariants, α_{ij} — the internal stress tensor as the linear function of the plastic prestrain tensor, R — the scalar parameter as the function of the plastic prestrain intensity, D_0, σ_0 and n — the material constants dependent on the temperature and creep stress level.

CALLADINE, DRUCKER [15] introduced the relation

$$D_{ij} = \frac{\partial \Psi}{\partial \sigma^c_{ij}}, \qquad \Psi = \frac{\sigma_0 D_0}{n+1} \Phi^{n+1}, \tag{3}$$

where the dimensionless function Φ is homogeneous of degree one in space σ^c_{ij}/σ_0 and has a value unity when σ^c_{ij} is the uniaxial tension. The surfaces of the constant Φ in the stress space for an isotropic body are convex, similar, concentric and represent constant rates of dissipation. The steady-state creep rate tensor is normal to each surface at the appropriate stress point.

For an isotropic material and for steady-state creep condition, the following relation is fulfilled [15]:

$$\Phi^{n+1} \equiv \Lambda \equiv \Lambda(\sigma^c_{ij}/\sigma_0) = (\sigma^c_i/\sigma_0)^{n+1}, \tag{4}$$

where the surface defined by the equation

$$\Phi = \sigma^c_i/\sigma_0 = \text{const} \tag{5}$$

is called "the creep plastic potential".

For an isotropic body and plane creep stress conditions the creep plastic potential has the form

$$\Phi = \{[(\sigma^c_{11})^2 - \sigma^c_{11}\sigma^c_{22} + (\sigma^c_{22})^2 + 3(\sigma^c_{12})^2]/\sigma_0^2\}^{1/2} = \text{const} \tag{6}$$

and for fixed 11 and 12 directions, Eq. (6) is geometrically represented in the creep stress level space σ^c_{11}/σ_0, σ^c_{22}/σ_0, σ^c_{12}/σ_0 by an ellipsoid [4, 5], the different ways of loading, usually considered in the plane creep stress experiments, are represented by ellipses lying on the surface of the appropriate ellipsoid.

For a material with strain-induced anisotropy the creep plastic potential surfaces are subjected to the complex shape deformation. This effect can be described as both translation to a new location and an expansion of the surface in the creep stress space σ^c_{ij}/σ_0.

The constitutive equation based on the notation of creep plastic potential for strain-induced anisotropic materials has the form (2) where

$$\Phi = \frac{[(3/2)\,(S^c_{ij}-\alpha_{ij})\,(S^c_{ij}-\alpha_{ij})]^{1/2}}{R\sigma_0} \tag{7}$$

and

$$\alpha_{ij} = A\int de^p_{ij}, \qquad R = 1+C\left[\int de^p_i\right]^r. \tag{8}$$

For experimental conditions, Eq. (2) has the evident form

$$\frac{D^\theta_{11}}{D_0} = \frac{\left[\left(\sigma^c_{11}-\frac{3}{2}Ae^p_i\cos\theta^p\right)^2+3\,(Ae^p_i\sin\theta^p)^2\right]^{\frac{n-1}{n}}}{\{[1+C\,(e^p_i)^r]\,\sigma_0\}^n}\times \tag{9}$$

$$\times\left(\sigma^c_{11}-\frac{3}{2}Ae^p_i;\cos\theta^p\right),$$

where A, C and r denote the material constants dependent on plastic prestrain history.

The influence of strain-induced material anisotropy on steady-state creep rate using tensor functions representations can be described in the following general form [7]:

$$D_{ij} = f\,(S^c_{ij}, Q^p_{ij}), \tag{10}$$

where Q^p_{ij} denotes the tensor parameter as the deviatoric part of the strain-induced tensor.

The authors [7] proposed the linear tensor relation

$$D_{ij} = \varphi_1\,S^c_{ij}+\varphi_2\,(S^c_{ki}\,Q^p_{jk}+Q^p_{li}\,S^c_{jl}), \tag{11}$$

where φ_i, for $i=1, 2$, is the scalar function of second invariants of the tensors S^c_{ij} and Q^p_{ij}.

For current experimental conditions, where the tensors S^c_{ij} and Q^p_{ij} can be shown as

$$S^c_{ij} = \begin{vmatrix} \frac{2}{3}\sigma^c_{11}, & 0, & 0 \\ 0, & -\frac{1}{3}\sigma^c_{11}, & 0 \\ 0, & 0, & -\frac{1}{3}\sigma^c_{11} \end{vmatrix}, \quad Q^p_{ij} = \begin{vmatrix} e^p_{11}, & e^p_{12}, & 0 \\ e^p_{12}, & -\frac{1}{2}e^p_{11}, & 0 \\ 0, & 0, & -\frac{1}{2}e^p_{11} \end{vmatrix} \tag{12}$$

the scalar function φ_2 in Eq. (11) is equal to zero.

For this purpose the authors [7] introduced the simple law

$$\frac{D_{ij}}{D_0} = \left[\frac{\sqrt{\mathrm{tr}\,(S^c_{ij})^2}}{\sigma_0}\right]^{n-1} \{1 - B\,[\sqrt{\mathrm{tr}\,(Q^p_{ij})^2}\,]^m\}\,(S^c_{ij} - \beta Q^p_{ij}). \tag{13}$$

Equation (13) is comparable with the form (2) by introducing the parameters

$$\alpha_{ij} = \beta Q^p_{ij} \quad \text{and} \quad R = \frac{1}{1 - B\,[\sqrt{\mathrm{tr}\,(Q^p_{ij})^2}\,]^m}. \tag{14}$$

The constitutive equation (13) has the evident form

$$\frac{D^\theta_{11}}{D_0} = \left(\frac{\sigma^c_i}{\sigma_0}\right)^{n-1} [1 - B\,(e^p_i)^m]\,(S^c_{11} - \beta e^p_i \cos\theta^p)/\sigma_0, \tag{15}$$

where B, β and m denote material constants dependent on plastic prestrain history.

5. Comparison

The aim of the experimental part of the work was to measure the values of steady-state creep rates for a material with room temperature biaxial strain-induced anisotropy.

The two presented theoretical approaches have the common description using two internal state variables, Eq. (2).

The basic material constants $\sigma_0 = 294$MPA, $n = 3$ and $D_0 = 0.9 \cdot 10^{-6}\,\mathrm{h}^{-1}$ were appointed from uniaxial creep tests at 300°C. The remaining material constants $A = 50.5$MPa for $e^p_i = 3\%$, $A = 37.5$MPa for $e^p_i = 7\%$, $C = 0.1$ and $r = 0.26$ — Eq. (9) and $B = -1$, $\beta = 1.47$MPa and $m = -6.45 \cdot 10^{-2}$ — Eq. (15) were appointed from the experimental values of steady-state creep rates with simple anisotropy which has been induced in axial tension and pure torsion directions exactly by using the three values with the angles $\theta^p = 0^0$ and $\theta^p = 90°$ under $e^p_i = 7\%$ and $\theta^p = 90°$ under $e^p_i = 3\%$.

In Eq. (9) the kinematic hardening tensor parameter α_{ij} is not directly proportional to the magnitude of plastic prestrain e^p_i. It was found by Ziegler (16) that the parameter A in the case of nonlinear kinematic hardening is the function of load history.

The experimental values of steady-state creep rates (as the functions of the angle θ^p and magnitude e^p_i) and theoretical curves appointed from Eq. (9) (interruption line) and Eq. (15) were compared in plots, Fig. 6.

The two theoretical approaches have an equal number of material constants and the same degree of accuracy describing the phenomenon discussed below, Fig. 6.

As it was mentioned, room temperature plastic prestrain causes creep

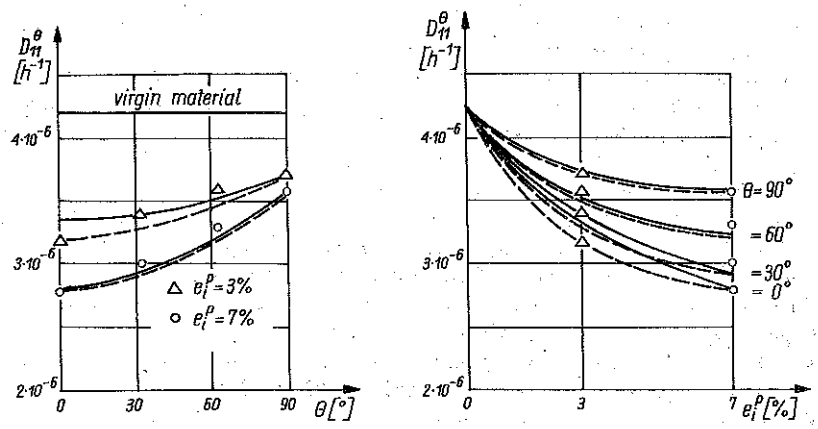

Fig. 6. Comparison of experimental data with two theoretical approaches.
— — — — theoretical description — Eq. (9),
———— theoretical description — Eq. (15),
○ △ experimental data.

strengthening of pure copper at 300°C. The current investigation has shown that the steady-state creep rate is decreased and the creep hardening depends simultaneously on the value and direction of plastic prestrain.

The influence of the hardening parameters α_{ij} and R on steady-state creep rate is different depending on the direction and value of plastic prestrain. For $\theta^p = 90$, the axial steady-state creep rate D_{11}^{90} exclusively depens on the scalar parameter R, Eqs. (9) and (15).

The significance of kinematic hardening in steady-state creep rate description is maximal for the case where the direction of plastic prestrain was in compliance to the creep direction, $\theta^p = 0^0$ and gradually decreasing with the increase of the value of angle θ^p.

References

1. B. F. Dyson, M. J. Rodgers, *Prestrain, cavitation and creep ductility*, Metal Sci., **8**, 261, 1974.
2. B. F. Dyson, M. S. Loveaday, M. J. Rodgers, *Grain boundary cavitation under various states of applied stress*, Proc. R. Soc. Lond. A, **349**, 245, 1976.
3. D. R. Hayhurst, W. A. Trampczyński, F. A. Leckie, *Creep rupture under non-proportional loading*, Acta Metall., **28**, 1171, 1980.
4. W. A. Trampczyński, *The influence of cold work on the creep of copper under biaxial states of stress*, Acta Metall., **30**, 1035, 1982.
5. W. Szczepiński, *On the effect of plastic deformation on yield condition*, Arch. Mech., **15**, 2, 1963.
6. J. R. Rice, *On the surface of stress-strain relations for time dependent plastic deformation in metals*, J. Appl. Mech., **37**, 728, 1970.

7. A. SAWCZUK, W. A. TRĄMPCZYŃSKI, *A theory of anisotropic creep after plastic prestraining*, Int. J. Mech. Sol., **24**, 647, 1982.
8. J. P. BOEHLER, A. SAWCZUK, *On yielding of oriented solids*, Acta Mech. **27**, 185, 1977.
9. N. S. MOZAROWSKI, J. A. ANTIPOW, N. I. BOBYR, *Creep and life-time of materials under programing loads* [in Russian], Kiev 1982.
10. M. WANIEWSKI, *The influence of direction and value of plastic prestrain on creep in metals*, Doctoral Thesis [in Polish], IFTR Reports, 34, 1983.
11. A. A. IL'YUSHIN, *Plasticity* [in Russian], A.N.USSR, Moscow 1963.
12. Y. OHASHI, M. TOKUDA, H. YAMASHITA, *Effect of third invariant of stress deviator on plastic deformation of mild steel*, J. Mech. Phys. Solids, **23**, 295, 1975.
13. A. MILLER, *An inelastic constitutive model for monotonic, cyclic and creep deformation*, J. Engeng. Mat. Tech.-Trans. ASME-H, **98**, 97, 1976.
14. A. R. S. PONTER, F. A. LECKIE, *Constitutive relationships for the time-dependent deformation in metals*, J. Engeng. Mat. Tech.-Trans. ASME-H, **98**, 47, 1976.
15. C. R. CALLADINE, D. C. DRUCKER, *Nesting surface of constant rate of energy dissipation in creep*, Q. Appl. Math., **20**, 79, 1962.
16. H. ZIEGLER, *A modification of Prager's hardening rule*, Q. Appl. Math., **17**, 55, 1959.

STRESZCZENIE

WPŁYW KIERUNKU I WARTOŚCI WSTĘPNEJ DEFORMACJI PLASTYCZNEJ NA USTALONĄ PRĘDKOŚĆ PEŁZANIA PRZY ZASTOSOWANIU ZŁOŻONEGO IZOTROPOWO-KINEMATYCZNEGO PRAWA WZMOCNIENIA

Oddziaływanie zmiany kierunku i wartości wstępnej deformacji plastycznej przeprowadzonej w temperaturze pokojowej na ustaloną prędkość pełzania badano eksperymentalnie na cienkościennych próbkach rurkowych wykonanych z czystej miedzi i poddanych działaniu złożonych stanów obciążenia, tzn. siły osiowej i skrętnej. Weryfikowano równanie konstytutywne, wprowadzając dwa różne podejścia — pojęcie plastycznego potencjału pełzania oraz własności reprezentacji funkcji tensorowych.

РЕЗЮМЕ

ВЛИЯНИЕ НАПРАВЛЕНИЯ И ЗНАЧЕНИЯ ВСТУПИТЕЛЬНОЙ ПЛАСТИЧЕСКОЙ ДЕФОРМАЦИИ НА УСТАНОВЛЕННУЮ СКОРОСТЬ ПОЛЗУЧЕСТИ ПРИ ПРИМЕНЕНИИ СЛОЖНОГО ИЗОТРОПНО-КИНЕМАТИЧЕСКОГО ЗАКОНА УПРОЧНЕНИЯ

Воздействие изменения направления и значения вступительной пластической деформации, проведенной в комнатной температуре, на установленную скорость ползучести исследовано экспериментально на тонкостенных трубчатых образцах, изготовленных из чистой меди, и подвергнутых действию сложных состояний нагружения, т.зн. осевой и скручивающей сил.

Проверено определяющее уравнение, вводя два разных подхода — понятие пластического потенциала ползучести и свойства представлений тензорных функций.

POLISH ACADEMY OF SCIENCES
INSTITUTE OF FUNDAMENTAL TECHNOLOGICAL RESEARCH.

Received March 27, 1984.